



# Simplified extended Kalman filter phase noise estimation for CO-OFDM transmissions

TU T. NGUYEN,<sup>1,3,\*</sup> SON T. LE,<sup>2</sup> MARC WUILPART,<sup>1</sup>  
TATIANA YAKUSHEVA,<sup>3</sup> AND PATRICE MÉGRET<sup>1</sup>

<sup>1</sup>Faculté Polytechnique - Université de Mons, Boulevard Dolez 31, 7000 Mons, Belgium

<sup>2</sup>Nokia Bell Labs, Stuttgart, Germany

<sup>3</sup>Proximus SA, Koning Albert II laan 27B, 1030 Brussels, Belgium

\*[tuthanh.nguyen@umons.ac.be](mailto:tuthanh.nguyen@umons.ac.be)

**Abstract:** We propose a flexible simplified extended Kalman filter (S-EKF) scheme that can be applied in both pilot-aided and blind modes for phase noise compensation in 16-QAM CO-OFDM transmission systems employing a small-to-moderate number of subcarriers. The performance of the proposed algorithm is evaluated and compared with conventional pilot-aided (PA) and blind phase search (BPS) methods via an extensive Monte Carlo simulation in a back-to-back configuration and with a dual polarization fiber transmission. For 64 subcarrier 32 Gbaud 16-QAM CO-OFDM systems with 200 kHz combined laser linewidths, an optical signal-to-noise ratio penalty as low as 1 dB can be achieved with the proposed S-EKF scheme using only 2 pilots in the pilot-aided mode and just 4 inputs in the blind mode, resulting in a spectrally efficient enhancement by a factor of 3 and a computational effort reduction by a factor of more than 50 in comparison with the conventional PA and the BPS methods, respectively.

© 2017 Optical Society of America under the terms of the [OSA Open Access Publishing Agreement](#)

**OCIS codes:** (060.1660) Coherent communications; (060.2330) Fiber optics communications; (060.4080) Modulation.

## References and links

1. S. Chandrasekhar and X. Liu, "OFDM based superchannel transmission technology," *J. Lightw. Tech.* **30**, 3816–3823 (2012).
2. D. S. Millar, R. Maher, D. Lavery, T. Koike-Akino, M. Pajovic, A. Alvarado, M. Paskov, K. Kojima, K. Parsons, B. C. Thomsen, S. J. Savory, and P. Bayvel, "Design of a 1 Tb/s superchannel coherent receiver," *J. Lightwave Technol.* **34**, 1453–1463 (2016).
3. Q. Zhuge, M. H. Morsy-Osman, and D. V. Plant, "Low overhead intra-symbol carrier phase recovery for reduced-guard-interval CO-OFDM," *J. Lightwave Technol.* **31**, 1158–1169 (2013).
4. S. T. Le, P. A. Haigh, A. D. Ellis, and S. K. Turitsyn, "Blind Phase Noise Estimation for CO-OFDM Transmissions," *J. Lightwave Technol.* **34**, 745–753 (2016).
5. Q. Zhuge, X. Xu, M. E. Mousa-Pasandi, M. Morsy-Osman, M. Chagnon, Z. A. El-Sahn, and D. V. Plant, "Experimental study of the intra-channel nonlinearity influence on single-band 100G coherent optical OFDM systems," *IEEE Photon. Tech. Lett.* **25**, 553–555 (2013).
6. S. Cao, P. Y. Kam, and C. Yu, "Decision-aided, pilot-aided, decision-feedback phase estimation for coherent optical OFDM systems," *IEEE Photon. Tech. Lett.* **24**, 2067–2069 (2012).
7. S. T. Le, T. Kanesan, E. Giacomidis, N. J. Doran, and A. D. Ellis, "Quasi-pilot aided phase noise estimation for coherent optical OFDM systems," *IEEE Photon. Tech. Lett.* **26**, 504–507 (2014).
8. T. Pfau, S. Hoffmann, and R. Noé, "Hardware-efficient coherent digital receiver concept with feedforward carrier recovery for M-QAM constellations," *J. Lightwave Technol.* **27**, 989–999 (2009).
9. M. Zamani, H. Najafi, D. Yao, J. Mitra, X. Tang, C. Li, and Z. Zhang, "Trellis-based feed-forward carrier recovery for coherent optical systems," *Opt. Express* **24**, 23531–23542 (2016).
10. M. Zamani, H. Najafi, D. Yao, J. Mitra, C. Li, and Z. Zhang, "Method and apparatus for residual phase noise compensation," Google Patents **US9537683**, 2017.
11. S. T. Le, M. E. McCarthy, N. M. Suihne, P. a. Haigh, E. Giacomidis, N. J. Doran, A. D. Ellis, and S. K. Turitsyn, "Decision Directed Free Blind Phase Noise Estimation for CO OFDM," *Optical Fiber Communication Conference (OFC)* **8724**, W1E.5 (2015).
12. D. Zibar, L. H. H. De Carvalho, M. Piels, A. Doberstein, J. Diniz, B. Nebendahl, C. Franciscangelis, J. Estaran, H. Haisch, N. G. Gonzalez, J. C. R. De Oliveira, and I. T. Monroy, "Application of machine learning techniques for amplitude and phase noise characterization," *J. Lightwave Technol.* **33**, 1333–1343 (2015).
13. L. Pakala and B. Schmauss, "Extended Kalman filtering for joint mitigation of phase and amplitude noise in coherent QAM systems," *Opt. Express* **24**, 6391–6401 (2016).

14. T. H. Nguyen and C. Peucheret, "Kalman filtering for carrier phase recovery in optical offset-QAM Nyquist WDM systems," *IEEE Photon. Tech. Lett.* **29**, 1019–1022 (2017).
15. J. Armstrong, "OFDM for Optical Communications," *J. Lightwave Technol.* **27**, 189–204 (2009).
16. O. V. Sinkin, R. Holzlöhner, S. Member, J. Zweck, and C. R. Menyuk, "Optimization of the Split-Step Fourier Method in Modeling Optical-Fiber Communications Systems," *J. Lightwave Technol.* **21**, 61–68 (2003).
17. L. Tomba, "On the effect of Wiener phase noise in OFDM systems," *IEEE Transactions on Communications* **46**, 580–583 (1998).
18. Ronen Dar, Meir Feder, Antonio Mecozzi and Mark Shtaif, "Accumulation of nonlinear interference noise in fiber-optic systems," *Opt. Express* **12**, 14199–14211 (2014).
19. S. T. Le, M. E. McCarthy, N. M. Suibhne, P. A. Haigh, E. Giacoumidis, N. J. Doran, A. D. Ellis, and S. K. Turitsyn, "Multiplier-free Blind Phase Noise Estimation for CO-OFDM Transmission," *European Conference on Optical Communication (ECOC)*, 1–3 W1E.5 (2015).
20. R.-J. Essiambre, G. Kramer, P. J. Winzer, G. J. Foschini, and B. Goebel, "Capacity Limits of Optical Fiber Networks," *J. Lightwave Technol.* **28**, 662–701 (2010).

## 1. Introduction

To meet the ever increasing demand for capacity, in the last decade, two high spectral efficiency (SE) advanced modulation techniques, namely Nyquist pulse shaping (NPS) and orthogonal frequency division multiplexing (OFDM), together with dense wavelength division multiplexing (WDM) have been intensively investigated for coherent optical (CO) communications [1, 2]. Compared to single carrier NPS based transmissions, the multicarrier OFDM approach shows excellent tolerance towards residual linear fiber impairments such as residual chromatic dispersion (CD) and polarization mode dispersion (PMD) while requiring a simple (one tap) equalization at the receiver. These features make OFDM transmission an attractive candidate for future optical networks. On the other hand, the CO-OFDM transmission also suffers from serious drawbacks. Due to relatively long symbol durations, CO-OFDM is much more vulnerable to phase noise (PN) which mainly originates from imperfect lasers at both transmitter and receiver. Both common phase error (CPE) and inter-carrier interference (ICI), introduced by the PN, result in severe performance degradations as orthogonality is no longer ensured in CO-OFDM systems [1]. To increase the PN tolerance, shorter OFDM symbol duration (lower number of subcarrier) is desirable. This can be achieved in reduced-guard-band or even zero-guard-band OFDM thanks to the fast development in digital signal processing (DSP) for fiber linear compensation techniques [3]. In this scenario, the influence of PN on CO-OFDM system performance is dominated by the CPE rather than ICI [3, 4]. In addition, it has been shown that reducing the number of subcarriers effectively increases the transmission performance of multi-carrier systems due to the reduction of nonlinear impairments [5]. As a result, for suppressing both nonlinear and laser phase noise impairments in OFDM transmissions with small-to-moderate number of subcarriers is of great interest.

There have been several techniques in the literature to deal with CPE [3, 4, 6, 7]. The most widely approach is pilot-aided (PA) technique due to its simplicity. By transmitting several pre-known patterns (or pilots) in each OFDM symbol, the CPE can be estimated easily and efficiently in term of low computational efforts. However, this method is coming at the cost of SE loss as some subcarriers are not used to carry useful data. To increase SE while keeping the simple implementation of PA method, authors in [7] proposed a technique called quasi-pilot aided estimation in which first half pilot subcarriers are data modulated and the second half subcarriers are the complex conjugate of the first one. This techniques reduces pilot overhead by the factor of two while keeping the same performance as in the conventional PA method. To further increase SE, several blind phase noise estimation (PNE) techniques have been proposed in the literature. For instance, authors in [8] proposed the blind phase search (BPS) direct decision (DD) method for single carrier transmission and its modification - the BPS decision directed free (DDF) technique in [4] was developed for CO-OFDM. More recently, a trellis-based phase correction has been proposed for single carrier transmission but its applications for multicarrier

systems have not been carried out [9, 10]. In general, the complexity of blind PNE is higher than that of pilot based methods by a factor of hundreds or even thousands [4]. They normally require phase tracking circuit operating either in feedback loop (FL) or in digital phase tracking manner to avoid phase uncertainty issues in CO-OFDM [4]. Moreover, several blind phase estimation techniques also suffer from strong performance degradation due to the small number of input data (for complexity requirement), which cannot exceed the number of subcarriers [4, 11]. As a result, existing phase noise compensation approaches, such as PA, BPS, and decision-directed-free blind, are not very efficient for OFDM transmission with small-to-moderate number of subcarriers (16~200) due to high overhead and high computational complexity, respectively.

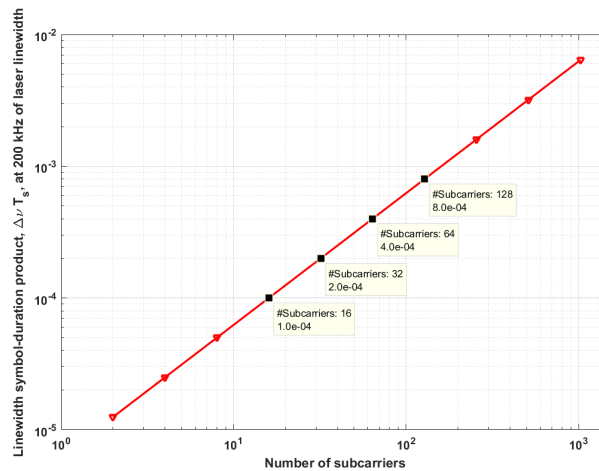


Fig. 1. Linewidth symbol-duration product,  $\Delta\nu T_s$ , as a function of number of subcarriers at 200 kHz combined laser linewidth for 32 Gbaud CO-OFDM transmission.

In the framework of Bayesian filtering, the Kalman filter has provided optimal laser phase characterization and tracking for single carrier [12, 13] and phase noise suppression for offset quadrature amplitude modulation (OQAM) based Nyquist WDM CO transmission systems [14]. These Kalman models showed an excellent PN tracking capability under low linewidth symbol-duration products (called normalized linewidth (NLW) for short), which, unfortunately, is not the case of  $\sim 32$  Gbaud CO-OFDM systems with more than 16 subcarriers under current commercial external cavity laser (ECL) linewidth requirement ( $\sim 100$  kHz). Figure 1 shows equivalent NLWs at 200 kHz combined laser linewidth (combined linewidths of transmit laser and local oscillator, 100 kHz each) when the number of subcarriers changes for 32 Gbaud CO-OFDM systems. It is easily observed that the NLW requirement for more than 16 subcarriers CO-OFDM transmissions should be above  $1.0 \times 10^{-4}$  while with modified Kalman model in [14], the obtained NLW was below  $6.0 \times 10^{-5}$  for less than 1 dB optical signal to noise ratio (OSNR) penalty at the bit-error-rate (BER) threshold of  $3.8 \times 10^{-3}$  for 16-OQAM Nyquist based WDM systems.

In order to improve the Kalman based PN estimation for such CO-OFDM systems, we propose in this paper, for the first time, a flexible (operating in pilot-aided and blind modes) simplified extended Kalman filter (S-EKF) scheme in which the number of inputs for Kalman are adjustable according to performance requirements. As opposed to the modified Kalman schemes in [13] or [14] in which both amplitude and phase noises can be tracked simultaneously, the inputs of our S-EKF are pure angular quantities and thus, the computational complexity is decreased approximately by a factor of four. We target the S-EKF for blind PN estimation (in blind mode operation). However, under some certain conditions, the S-EKF is suggested to operate in the pilot-aided mode with the advantage of providing better performance than in the conventional

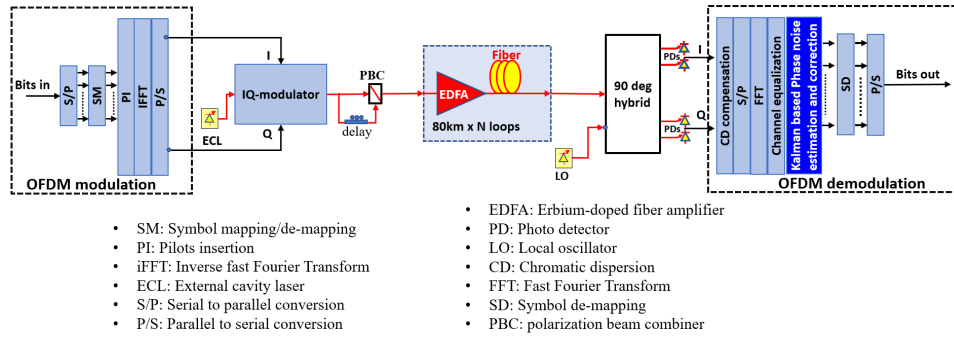


Fig. 2. Block diagram of CO-OFDM with phase noises from lasers and fiber nonlinearity during optical fiber transmission.

PA method with lower pilot overhead. The performance of S-EKF is numerically validated for 16-quadrature amplitude modulation (QAM) CO-OFDM system with the number of subcarriers varied from 32 to 96. For a fair comparison, their performances are compared to the conventional PA method in the pilot-aided mode and the BPS DD-FL technique in the blind mode.

## 2. CO-OFDM transmission modeling and parameters

The principle and basic block diagram of CO-OFDM transmission, as shown in Fig. 2, have been well-studied in various publications [3, 4, 15]. We adopt a similar design for our studies with emphasis on PN estimation and correction employing the Kalman filtering theory. As shown in Fig. 2, the 32 Gbaud OFDM signal on each polarization is generated from multiple 16-QAM streams by using inverse fast Fourier transform (iFFT) (net data rate of 119 Gb/s after 7% hard-decision forward error correction (HD-FEC) overhead). The number of subcarriers is changed between 32, 64, and 96 while the number of pilot subcarriers is varied from 2 to 12. The time domain in-phase (I) and quadrature (Q) components of OFDM signals after iFFT are then converted to optical domain via an ideal in-phase quadrature (IQ) modulator.

Without loss of generality, dual polarization transmission (using the Manakov system without taking into account state of polarization, PMD and polarization dependent loss [16]) is simulated while one polarization is detected and demodulated with a coherent reception at the receiver for simplicity (i.e. only cross-polarization impairment is considered). We assume that there are no synchronization and frequency offset errors. The long-haul optical link consists of multiple spans of 80 km standard single-mode fiber (SSMF) in which Erbium-doped fiber amplifier (EDFA) are used to compensate fiber losses. Each in-line EDFA with 6 dB of noise figure (NF) adds some amplified spontaneous emission (ASE) noise which is accumulated along fiber propagation and considered as an additive white Gaussian noise process. Following parameters of the SSMF are: fiber loss coefficient  $\alpha = 0.2 \text{ dB km}^{-1}$ , dispersion coefficient  $\beta_2 = -2.0 \times 10^{-26} \text{ s}^2 \text{ m}^{-1}$  (corresponding to the fiber dispersion of  $17 \text{ ps km}^{-1} \text{ nm}^{-1}$  at the reference wavelength of 1550 nm) and nonlinear Kerr coefficient  $\gamma = 1.2 \text{ W}^{-1} \text{ km}^{-1}$ . The electric field complex envelop of a traveling light wave are mathematically well-described by the nonlinear Schrödinger equations and the well-known symmetric split-step Fourier method is used to model the signal propagation in fiber channels [16].

The laser PN,  $\Phi(t)$ , is introduced either by ECL at the transmitter or local oscillator (LO) at the receiver sides, and it can be modeled as a Wiener random process. The PN model in CO-OFDM can be written in the discrete form as [4, 17]

$$\Phi(m) = \Phi(m-1) + \nu(m), \quad (1)$$

where  $\nu(m) \sim \mathcal{N}(0, 2\pi\Delta\nu T_s)$  with  $\Delta\nu$  being the laser linewidth and  $T_s$  being the OFDM period.

For convenience, the laser linewidth of LO at the receiver is assumed to be identical with ECL's linewidth at the transmitter. Thus, the combined laser linewidth is two times of ECL's linewidth.

Mathematically, the  $m^{th}$  time domain OFDM symbol at the transmitter (after iFFT) can be written as

$$\begin{aligned} x_m(n) &= \mathcal{F}^{-1}(X_{m,k}) \\ &= \sum_{k=0}^{N-1} X_{m,k} \exp\left(j2\pi \frac{kn}{N}\right), \quad mN \leq n < (m+1)N, \end{aligned} \quad (2)$$

with  $X_{m,k}$  and  $N$  being the transmitted QAM symbol at the  $m^{th}$  symbol, on the  $k^{th}$  subcarrier, and the number of subcarriers, respectively.

At the reception side, the incoming optical signal is first converted into the equivalent baseband signal in the electrical domain by an ideal coherent receiver. Taking into account the ASE noise from amplifiers, CD and PN, the received OFDM signal can be written as

$$y_m(n) = \exp(j\phi_m(n)) \left( x_m(n) \otimes \mathcal{F}^{-1}(H_m(k)) \right) + w_m(n), \quad (3)$$

where  $\otimes$  and  $\mathcal{F}^{-1}(\cdot)$  denote circular convolution and iFFT operators, respectively.  $\phi_m(n)$  is the instantaneous phase noise at the  $m^{th}$  OFDM symbol and at the  $n^{th}$  time index.  $w_m(n)$  is ASE which is considered as Gaussian noise.  $H_m(k)$  is the channel response at the  $k^{th}$  subcarrier. It is nothing but the function of CD in frequency domain as

$$H(z, \omega) = \exp\left(-j \frac{D\lambda^2 z}{4\pi c} \omega^2\right), \quad (4)$$

where  $\omega$  is the angular frequency,  $z$  is the transmission distance,  $D$  is the fiber chromatic dispersion parameter,  $c$  is the speed of light and  $\lambda$  is the carrier wavelength. The effect of CD is compensated totally by the "CD compensation" block (simply the inversion of CD response), placed before OFDM demodulation. Thus, no cyclic prefix is needed in our system. The received signal in the frequency domain at the receiver can be obtained by taking the fast Fourier transform (FFT) operator of the signal after CD compensation, as

$$\begin{aligned} Y_m(k) &= \mathcal{F}\left(y_m(n) \otimes \mathcal{F}^{-1}\left(H_m(k)^{-1}\right)\right) \\ &= X_m(k)I_m(0) + \text{ICI}_m(k) + W_m(k), \end{aligned} \quad (5)$$

where the  $\text{ICI}_m(k)$  term is defined as

$$\text{ICI}_m(k) = \sum_{l=0, l \neq k}^{N-1} X_m(l)I_m(l-k), \quad (6)$$

and  $I_m(k)$  is given

$$I_m(k) = \frac{1}{N} \sum_{n=0}^{N-1} \exp(j\phi_m(n)) \exp\left(-j \frac{2\pi kn}{N}\right). \quad (7)$$

The term  $I_m(0)$  in the Eq. (5) is also known as CPE as it is simply the time-average of the phase noise deviation during one OFDM symbol

$$I_m(0) = \frac{1}{N} \sum_{n=0}^{N-1} \exp(j\phi_m(n)) \approx \exp(j\Phi(m)), \quad (8)$$

with  $\Phi(m)$  can also be understood as

$$\Phi(m) = \frac{1}{N} \sum_{n=0}^{N-1} \phi_m(n). \quad (9)$$

Thus, the orthogonality in OFDM is no longer maintained due to PN. The impact of PN from Eq. (5) can be characterized into two separate parts: the CPE which is a pure phase rotation from OFDM symbol to symbol and equal to the mean of the phase deviation, and the ICI which changes fast within one OFDM symbol. In reality, the CPE consists of laser phase noises (from ECL and LO) and average phase-shift due to the fiber nonlinearities (both self-phase modulation (SPM) and cross-phase modulation (XPM)) as a result of signal propagations through fibers [18]. In addition, residual channel fluctuations in CO-OFDM transmissions are always present due to various reasons such as residual CD. They are normally estimated and equalized by periodically inserting preamble sequences. Theoretically, we assume here that perfect channel equalization is available, i.e. the channel equalization block in our study acts as power normalization. Let  $R_m(k)$  be the signals after the channel equalization, we simply have  $E\{R_m(k)^2\} = 1$ , where  $E$  stands for expectation operator. This signal before going to the PN estimation and compensation is thus expressed in short as

$$R_m(k) = X_m(k)I_m(0) + \varepsilon_m(k),$$

where  $\varepsilon_m(k)$  is the so-called equalization-enhanced phase noise (EEPN) and given as

$$\varepsilon_m(k) = \text{ICI}_m(k) + W_m(k). \quad (10)$$

The EEPN term in the Eq. (10) is normally treated as a zero mean Gaussian noise [3, 4]. Equation (10) can be represented in PN distorted form as

$$R_m(k) = X_m(k) \exp(j\Phi(m)) + \varepsilon_m(k). \quad (11)$$

As stated in the introduction, the most widely used approach to estimate the CPE term is the PA technique due to its simplicity. By transmitting several pilots in each OFDM symbol, the CPE can be approximated as [3, 4, 6, 7]

$$\Phi(m) = \arg \left( \frac{1}{N_p} \sum_{l=1}^{N_p} \frac{R_m(l)X_m^*(l)}{|R_m(l)X_m(l)|} \right), \quad (12)$$

with  $N_p$  being the number of pilots. Clearly, the accuracy of CPE in Eq. (12) depends on the number of pilots used for the estimation at the cost of SE loss.

Our proposed S-EKF is placed after channel equalization for PN estimation and correction. The S-EKF can be operated in two modes: pilot-aided and blind modes and it is going to be described shortly afterward.

### 3. Simplified extended Kalman filter scheme for phase noise estimation

Let stack the  $m^{\text{th}}$  received symbols at pilot positions  $l_1, l_2, \dots, l_k$  with  $k \leq N$  as a vector  $\mathbf{R}_m^p = [R_{m,l_1}^p, R_{m,l_2}^p, \dots, R_{m,l_k}^p]^T$  and the corresponding transmitted symbols at pilot positions is  $\mathbf{A}_m^p = [X_{m,l_1}^p, X_{m,l_2}^p, \dots, X_{m,l_k}^p]^T$ . The received symbols at pilot positions can be presented in a matrix form as

$$\mathbf{R}_m^p = \mathbf{A}_m^p \exp(j\Phi_m) + \boldsymbol{\varepsilon}_m, \quad (13)$$

where  $\boldsymbol{\varepsilon}_m$  is a vector of EEPN terms at pilot positions which is characterized as Gaussian noise as mentioned above, and  $\Phi_m \triangleq \Phi(m)$  for a better Kalman illustration.

**Algorithm 1** Procedure of proposed S-EKF implementation.

- 1: Input:
    - phase noise observation  $\arg(\mathbf{R}_m^p)$ ,  $m = 1, 2, \dots$
    - noise matrices  $\mathbf{Q}$  and  $\mathbf{M}$
  - 2: initialization:
    - $\Phi_0 = 0$
    - $P_0 = 0$
  - 3: **for**  $m=1,2,3\dots$  **do**
  - 4:   *Prediction step*
  - 5:    $\hat{\Phi}_{m|m-1} = \Phi_{m-1}$  {priori state prediction}
  - 6:    $\hat{P}_{m|m-1} = P_{m-1} + \mathbf{Q}$  {error covariance prediction}
  - 7:   *Measurement update step*
  - 8:    $\arg(\hat{\mathbf{R}}_{m|m-1}^p) = \hat{\Phi}_{m|m-1} + \theta_m^{ref}$  {measurement expectation}
  - 9:    $\mathbf{e}_m = (\arg(\mathbf{R}_m^p) - \arg(\hat{\mathbf{R}}_{m|m-1}^p))$  {error calculation from the real measurement}
  - 10:    $\mathbf{G}_m = \hat{P}_{m|m-1} \mathbf{F}^T (\mathbf{F} \hat{P}_{m|m-1} \mathbf{F}^T + \mathbf{M})^{-1}$  {Kalman gain computation}
  - 11:    $\Phi_m = \hat{\Phi}_{m|m-1} + \mathbf{G}_m \mathbf{e}_m$  {update the prediction from Kalman gain and error}
  - 12:    $P_m = (1 - \mathbf{G}_m \mathbf{F}) \hat{P}_{m|m-1}$  {update the error covariance}
  - 13: **end for**
- $\mathbf{F}$  is simply the  $N_p \times 1$  unit matrix which originates from the fact  $\frac{\partial f}{\partial \Phi_m} |_{\Phi_m^p} = 1$ ,  $p = 1, 2, \dots, N_p$

The Eq. (1) and Eq. (13) can be seen as a set of process and measuring equations of a state space model (SSM) [12]. The phase variations  $\Phi_m$  is the state (hidden or non-observable) variable of the SSM that we desire to estimate while  $\mathbf{R}_m^p$  represents measurement (observable) variables which are the samples after OFDM demodulator at the coherent receiver. Due to the exponential component in the measurement equation, the linear Kalman filtering is not capable to apply directly, instead, an extended Kalman filtering is normally adopted in which the measurement is first linearized by taking the first derivative of the measurement with respect to phase variable [13, 14]. As a results, the complexity of those systems increases as all computations are needed to be calculated in the complex domain. In our S-EKF, we further transform the measurement quantities by taking the angular of measurement signals and put them as the inputs for S-EKF. Fortunately, the first derivative of the angular of received signals at pilot positions with respect to phase variable is simply a constant value and therefore, all the calculations can be done in the real field, resulting a significant computational effort reduction. More specifically, the angular of received symbols at pilots positions is

$$\begin{aligned} \arg(\mathbf{R}_m^p) &\approx \Phi_m + \theta_m^{ref} + \boldsymbol{\varepsilon}'_m \\ &= f(\Phi_m) + \boldsymbol{\varepsilon}'_m, \quad \text{where } f(\Phi_m) = \Phi_m + \theta_m^{ref}, \end{aligned} \quad (14)$$

with  $\theta_m^{ref}$  being the phase of transmitted QAM symbols which are assumed to be known in the pilot-aided mode and un-known in the blind mode at the receiver.  $f(\Phi_m)$  is denoted as observation function which maps the true state space into the observed space, and  $\boldsymbol{\varepsilon}'_m$  is the angular projection of  $\boldsymbol{\varepsilon}_m$  in the direction orthogonal to  $A_m^p \exp(j\Phi_m)$ . We rearrange the process and measurement equations according to the framework of Kalman filtering as following

$$\begin{aligned} \Phi(m) &= \Phi(m-1) + \nu(m) \\ \arg(\mathbf{R}_m^p) &= f(\Phi_m) + \boldsymbol{\varepsilon}'_m, \quad \text{where } f(\Phi_m) = \Phi_m + \theta_m^{ref}. \end{aligned} \quad (15)$$

Let  $\mathbf{Q}$  and  $\mathbf{M}$  be the covariance matrices of process and measurement noises respectively, i.e.  $\nu(m) \sim \mathcal{N}(0, \mathbf{Q})$  and  $\boldsymbol{\varepsilon}'_m \sim \mathcal{N}(0, \mathbf{M})$ , the CPE estimation can be tracked thanks to S-EKF

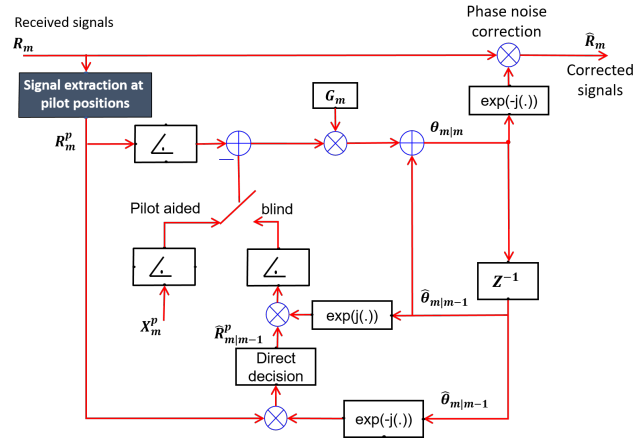


Fig. 3. Proposed S-EKF scheme phase noise estimation and correction for CO-OFDM transmission.

as shown in algorithm 1. To understand procedure of this algorithm, let us first define some conventional Kalman's terminologies. Variables with the subscripts  $m|m-1$  present a priori estimation (or prediction) for current state  $m$  while only having available measurements from one past state  $m-1$ . The subscripts  $m|m$  (or simply  $m$ ) is a posteriori estimation (or updates) when the current observation  $m$  is available. The core of Kalman filtering in the S-EKF scheme can be described as following: we first predict PN level at the time instant  $m$  from past measurement up to the time instant  $m-1$ . Once measurement at the time instant  $m$  is available, the error,  $e_m$ , is computed between the "true" state,  $\arg(R_m^p)$ , and the predicted states,  $\arg(\hat{R}_{m|m-1}^p)$ . This error is finally used to scale the Kalman gain before updating our prediction. In order to compute the error in step 9, the reference phases,  $\theta_m^{ref}$ , need to be available. They are normally coming from pre-known pilots. This scenario is the pilot-aided mode S-EKF. In the blind mode S-EKF, the reference phases are estimated blindly from the received signals together with predicted phase via a direct decision module. Its principle is understandable as received symbols tend to be distributed around their ideal locations in the constellation if the residual phase noise is small, i.e.  $[-\pi/4, \pi/4]$ . This assumption is necessary to avoid phase cycle-slip problem in a general blind phase estimation scheme [4]. The whole diagram of S-EKF operating in either pilot-aided or blind mode for CPE estimation and correction is shown in Fig. 3. Note that  $Q$  is a scalar in this case and its variance can be approximated from combined laser linewidth as  $2(2\pi\Delta\nu T_s)$ . The measurement noise correlation matrix,  $M$ , is a  $N_p \times N_p$  diagonal matrix in linear regime, i.e.  $M = \text{diag}(E(|\varepsilon'_{m,1}|^2), E(|\varepsilon'_{m,2}|^2), \dots, E(|\varepsilon'_{m,N_p}|^2))$ . As the measurement noise is proportional to OSNR and ICI terms, and it may also be changed due to the complicated interplay between ASE, CD and fiber nonlinearities, it is not always available for the Kalman algorithm execution in practice. Thus, we first estimate the measurement noise via training. As Kalman gain is updated every iteration from real observation rather than the noise parameters, the performance of S-EKF is not very sensitive to the accuracy of variance matrices. This is the well-known advantage of the Kalman filtering.

#### 4. Complexity analysis

In order to assess the complexity of S-EKF, we estimate the real-valued multiplications due to the fact that multipliers cost much more hardware resources than adders, subtractions and sign changes. For simplicity, one division is counted as one multiply operator. It should be noted that

Table 1. S-EKF computational analysis (from Algorithm 1) for CPE estimation.

		# of multiplications	note
Operation 5	$\hat{\Phi}_{m m-1} = \Phi_{m-1}$	0	
Operation 6	$\hat{P}_{m m-1} = P_{m-1} + Q$	0	
Operation 8	$\hat{\Phi}_{m m-1} + \theta_m^{ref}$	0	
Operation 9	$(\arg(\mathbf{R}_m^p) - \arg(\hat{\mathbf{R}}_{m m-1}^p))$	0	
Operation 10	$\mathbf{F} \hat{P}_{m m-1} \mathbf{F}^T + \mathbf{M}$	0	$\mathbf{F}$ is $N_p \times 1$ ones matrix
	$(\mathbf{F} \hat{P}_{m m-1} \mathbf{F}^T + \mathbf{M})^{-1}$	$\sum_{l=1}^{N_p} \frac{N_p!}{l!(N_p-l)!} + N_p^2 + 2$	The matrix for inversion contains only $N_p$ different numbers
	$\hat{P}_{m m-1} \mathbf{F}^T (\mathbf{F} \hat{P}_{m m-1} \mathbf{F}^T + \mathbf{M})^{-1}$	$\sum_{l=1}^{N_p} l$	The $(\cdot)_{N_p \times N_p}^{-1}$ is a symmetric matrix
Operation 11	$\Phi_m = \hat{\Phi}_{m m-1} + \mathbf{G}_m \mathbf{e}_m$	$N_p$	
Operation 12	$P_m = (1 - \mathbf{G}_m \mathbf{F}) \hat{P}_{m m-1}$	1	
Estimated total number of multiplication:		$\sum_{l=1}^{N_p} \frac{N_p!}{l!(N_p-l)!} + N_p^2 + \sum_{l=1}^{N_p} l + 3$	

there are normally four real-value multipliers to compute one complex-value multiply operation. It can be easily seen from the S-EKF flow chart that its complexity is  $O(n^3)$ , i.e. proportional to the cube of the inputs due to the matrix inversion operator while computing Kalman gain. Taking advantage of some special properties of simplified matrices in this case (see the note column in Table 1), it is expected that much complexity reduction can be obtainable, especially when the number of inputs is small (below 10). Table 1 summarizes step-by-step the number of real-value multiplications of the S-EKF. As shown in Fig. 3, there are  $8N_p$  more multiply operators when the S-EKF is operating at the blind mode due to two complex multipliers required for the phase rotations. These calculations are needed to figure out the predicted reference phases. It is worth noting that the phase rotations can be performed in polar coordinates using CORDIC algorithm without any multiplication [8, 19]. However, to make a fair comparison to other methods, we consider these phase rotations as multiply operators in the complex domain, and no CORDIC algorithm is taken into account. Thus, the total of real multiply operators from the Table 1 is slightly modified as

$$C_{S-EKF} = \sum_{l=1}^{N_p} \frac{N_p!}{l!(N_p-l)!} + N_p^2 + \sum_{l=1}^{N_p} l + 3 + 8N_p S_w, \quad (16)$$

where we denote  $S_w$  as a switch variable, i.e.  $S_w = 1$  when the S-EKF operates in the blind mode and  $S_w = 0$  when the S-EKF is in the pilot-aided mode.

As stated in the introduction, the state-of-the-art DDF method in [4, 11] cannot be applied for the CO-OFDM with relatively small number of subcarriers. Thus, we employed the BPS based DD as proposed in [8] but operating in a feedback manner as in [11] for comparison. In BPS DD-FL, the number of test phase for 16-QAM is fixed at 16 [4]. The number of test phase has a great impact on the overall complexity of BPS method and it has been shown in [4, 8] that it should be at least 16 for 16-QAM to obtain acceptable performances. To sum up, the complexity of our proposed pilot-aided and blind S-EKF schemes are compared with conventional PA and the BPS DD-FL methods, respectively, in terms of the number of real multiply operators as shown in the Table 2. The table suggests that the number of input data for the S-EKF in the pilot-aided

Table 2. Complexity comparison between S-EKF with conventional PA, and BPS DD-FL methods in term of the number of real multiply operators. All the results are based on no CORDIC implementation.

# inputs $N_p$	S-EKF (pilot-aided mode) Eq. (16), $S_w = 0$	Pilot aided $9 \times N_p$ Eq. (12)	S-EKF (blind mode) Eq. (16), $S_w = 1$	BPS DD with FL (16 test phases) $4 \times 16 \times N$
2	7	18	23	
4	24	36	56	$2048 _{N=32}$ ,
6	81	54	129	$4096 _{N=64}$ ,
8	286	72	350	$8192 _{N=128}$
10	1071	90	1151	

mode and in the blind mode should not be over 4 and 10 to maintain the competitiveness to the PA and BPS-DD methods, respectively, for a relatively same complexity and SE.

## 5. Results and discussions

To evaluate the performance of the S-EKF for PN estimation in CO-OFDM, we performed extensive simulation with at least  $10^6$  bits of transmission for error counting (100 repetitions, 100 OFDM symbols for each repetition). The DSP procedure after coherent receiver includes: CD compensation, serial-to-parallel conversion, OFDM demodulation using FFT, and channel equalization were employed implicitly. The 16-QAM demodulation, followed after PN estimation and compensation, converted complex data into bits. The received bits were compared with transmitted bits to estimate BER.

We first studied the behavior of the proposed S-EKF in back-to-back configuration in which the noise is a pure additive white Gaussian noise (AWGN) so that results can be compared against the theoretical limitation for 16-QAM as [20]

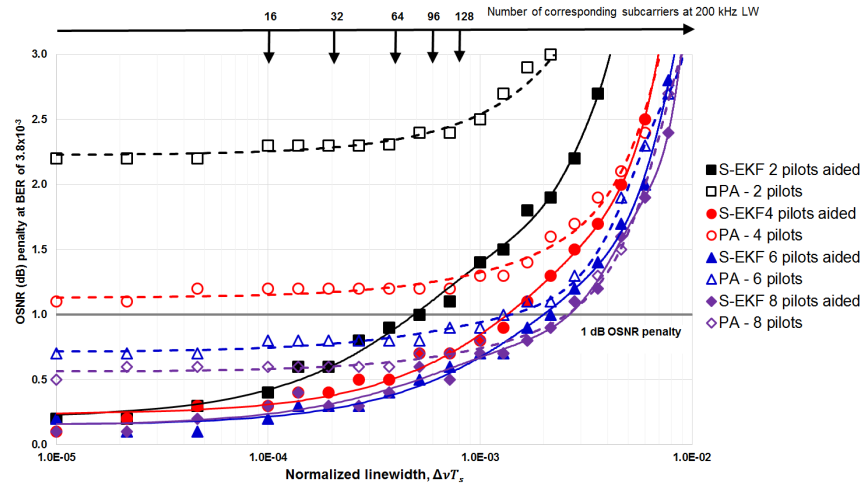
$$P_b = \frac{3}{8} \operatorname{erfc} \left( \sqrt{\frac{2\gamma_b}{5}} \right), \quad (17)$$

where  $\gamma_b$  is the signal to noise ratio (SNR) per bit and  $\operatorname{erfc}$  is the complementary error function. It should be noticed that the equivalent OSNR in one polarization with respect to the SNR per bit,  $\gamma_b$ , is

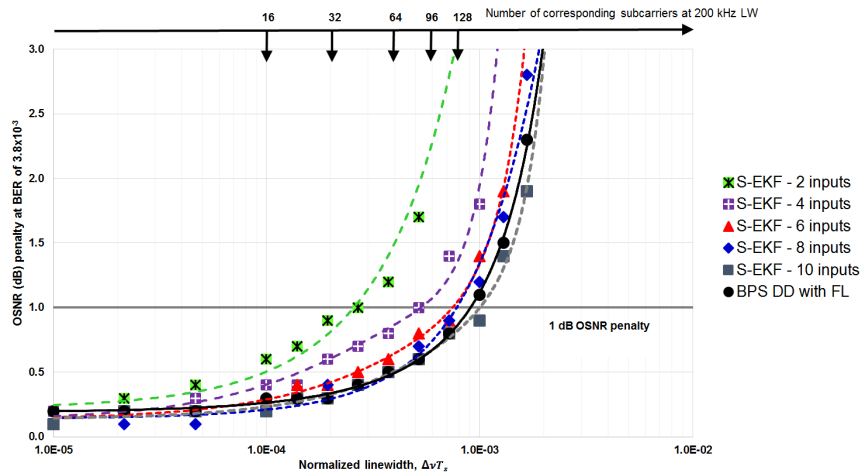
$$\text{OSNR} = \frac{R_b}{2B_{\text{ref}}} \gamma_b, \quad (18)$$

where  $R_b$  is the bit rate and  $B_{\text{ref}}$  is the reference bandwidth which is commonly chosen as 12.5 GHz. Common BER threshold before a typical 7% overhead HD-FEC is  $3.8 \times 10^{-3}$  [20]. The proposed pilot-aided and blind S-EKF algorithms were compared with conventional PA method and BPS DD-FL (16 test phases) for 32 Gbaud 16-QAM CO-OFDM transmissions (gross bit-rate of 128 Gb/s per polarization).

Figure 4 shows the comparison of the proposed S-EKF to the conventional PA in the pilot-aided mode [Fig. 4(a)] and to the BPS DD-FL in the blind mode [Fig. 4(b)] in terms of OSNR penalties against NLW for 64 subcarriers CO-OFDM transmissions. The OSNR penalties are the extra OSNRs with respect to theoretical OSNR expectation needed to achieve a BER of  $3.8 \times 10^{-3}$ . The theoretical OSNR expectation for 16-QAM 32 Gbaud signal at BER of  $3.8 \times 10^{-3}$  is  $\sim 16.2$  dB (derived from Eq. (17) and Eq. (18)). The equivalent NLWs for 32 Gbaud 16-QAM CO-OFDM at 200 kHz combined laser linewidth with different number of subcarriers are also provided in these figures for a better illustration and comparison. An acceptable of maximum 1 dB OSNR penalty is taken as threshold for comparison. It can be seen easily that the performances of the S-EKF are



(a) S-EKF compared with PA in pilot-aided mode under different number of pilots.



(b) S-EKF compared with DBP DD-FL in blind mode under different number of input data.

Fig. 4. A tolerant comparison against phase noise of the proposed S-EKF with PA and BPS DD-FL (direct decision based with feedback loop) for 32 Gbaud 16QAM CO-OFDM in back-to-back transmission. The vertical axis is OSNR penalty as a function of normalized linewidth at BER of  $3.8 \times 10^{-3}$  (7% HD-FEC threshold).

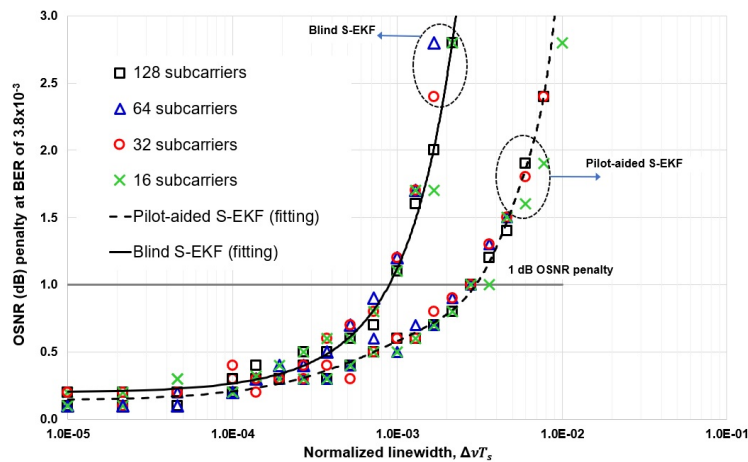


Fig. 5. Performance of 8 inputs S-EKF with different number of subcarriers for CO-OFDM.

always better than that of PA method in pilot-aided mode [Fig. 4(a)]. The largest advantages of S-EKF over PA are observed at smaller number of pilots and at lower NLWs. Below 1 dB OSNR penalty is never reached by PA method with less than 6 pilots while the S-EKF obtains even below 0.5 dB of OSNR penalty with only 2 pilots at  $\Delta\nu T_s \leq 2.0 \times 10^{-4}$  (corresponding to the systems of maximum 32 subcarriers). With 4 pilots, the CO-OFDM equipped with S-EKF can work well up to 128 subcarriers under 1 dB OSNR penalty constraint at 200 kHz combined laser linewidth. For 64 subcarriers transmission and under 1 dB OSNR penalty constraint, the 2 pilot-aided S-EKF obtains a similar performance to 6-pilot PA scheme at 200 kHz laser linewidth, showing an overhead reduction by a factor of 3 with slightly lower complexity than the PA. It can also be seen in this figure that there is not much advantage of S-EKF over conventional PA with more than 8 pilots. It is therefore more reasonable to employ S-EKF for around 64 subcarriers CO-OFDM with no more than 4 pilots to maintain low pilot overheads and outperformed performances.

By contrast, the system performance with S-EKF is approaching the BPS DD-FL method in the blind mode when the number of data is increasing as shown in Fig. 4(b). The performance of the proposed S-EKF is almost as the same as the BPS DD-FL with more than 6 inputs. Note that the performance of the BPS DD-FL method changes slightly with the number of subcarriers and the number of subcarriers should be larger than 32 to obtain a desired performance [4]. The BPS DD-FL performance, marked by black-rounded symbols, was simulated at 64 subcarriers. With 6 inputs, the S-EKF offers  $\sim 50$  time more computationally efficient than the BPS DD-FL method under 1 dB OSNR penalty constraint without significant performance degradations (less than 0.2 dB OSNR penalty difference). It is also very interesting to point out from this figure that the blind S-EKF obtains a remarkable NLW tolerance of  $\sim 8.0 \times 10^{-4}$  just using 6 to 8 inputs under 1 dB OSNR penalty constraint. This means that up to 128 subcarriers CO-OFDM can be realized under the combined laser linewidth of 200 kHz in the blind mode with an acceptable complexity. For systems less than 32 subcarriers, the proposed S-EKF is a good option as the BPS DD-FL is no longer working for such system. From these results, it is worth mentioning that the blind mode S-EKF with 6 to 8 input data is strongly suggested to implement for CO-OFDM transmission with no more than 96 subcarriers under combined laser linewidth of 200 kHz to achieve at the same time an acceptable OSNR penalty, moderate implementation complexity, and zero overhead due to pilots.

Another advantage of S-EKF is that its performance is independent of number of subcarriers which normally is not the case with other blind PN approaches for CO-OFDM [4]. This brings

great benefits for the implementation of CO-OFDM systems with small-to-moderate number of subcarriers. Figure 5 shows OSNR penalties at HD-FEC threshold of S-EKF in two operation modes as a function of NLW with different number of subcarriers. The number of subcarriers is varied from 16 to 128 in this simulation. It is easily seen that performances of S-EKF do not depend on the number of subcarriers in both operational modes. Both blind and pilot-aided S-EKF maintain the NLWs of  $8.0 \times 10^{-4}$  and  $3.0 \times 10^{-3}$ , respectively, under 1 dB OSNR penalty constraint at the HD-FEC threshold.

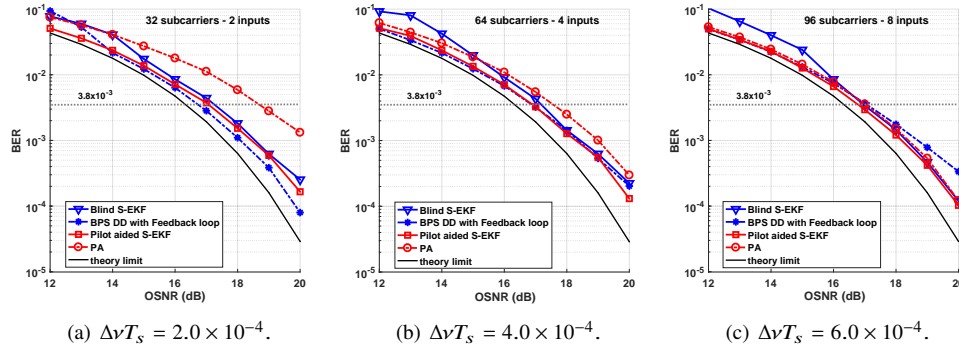


Fig. 6. BER as a function of OSNR for 32 Gbaud 16QAM CO-OFDM in back-to-back transmission at the same 200 kHz combined laser linewidth. The number of subcarriers and input data are 32/64/96 and 2/4/8, respectively.

Next, we conducted the simulation under different level of noise to see how the system equipped with S-EKF performed in comparison with the PA and BPS DD-FL methods in both pilot-aided and blind modes at 200 kHz combined laser linewidth. Figure 6 indicates the BER as a function of OSNR under some noticeable scenarios: 2 inputs for 32 subcarriers (i.e.  $\Delta\nu T_s = 2.0 \times 10^{-4}$ ) - Fig. 6(a), 4 inputs for 64 subcarriers (i.e.  $\Delta\nu T_s = 4.0 \times 10^{-4}$ ) - Fig. 6(b) and 8 inputs for 96 subcarriers (i.e.  $\Delta\nu T_s = 6.0 \times 10^{-4}$ ) - Fig. 6(c) CO-OFDM systems. As expected, systems equipped with S-EKF in both pilot-aided and blind mode clearly outperforms the PA when the number of inputs is small [Fig. 6(a)]. Only with 2 inputs, the performance of S-EKF is approaching the complicated BPS DD-FL method. When the number of data increases to 4 [Fig. 6(b)], the S-EKF still provides a better performance than the PA method in both modes at the HD-FEC threshold. Its performance in blind mode is almost identical to the complicated BPS DD-FL method. With 8 inputs, there is almost no difference between S-EKF, PA, and BPS DD-FL methods [Fig. 6(c)] at the HD-FEC threshold. The S-EKF with 8 data even outperforms the BPS DD-FL method at high OSNRs. In all cases, the S-EKF performs worse than the PA and BPS DD-FL methods at low OSNRs (i.e.  $\text{OSNR} \leq 15$  dB). This can be explained by the fact that the Kalman gain changes rapidly due to the incorrect error estimation after the direct decision process in Gaussian noise dominated environment. Thus, the proposed blind S-EKF is only adequate to apply for HD-FEC equipped systems, while the pilot-aided S-EKF can be employed for soft-decision forward error correction (SD-FEC) equipped transceivers.

Due to the fact that one of main issue of CO-OFDM is fiber nonlinearities, we evaluated the S-EKF performance versus the launched power with fiber transmission to see if there was any severe performance degradation. Bearing in mind that the fibers introduce some additional CPE which is defined as nonlinear average phase shift due to fiber Kerr nonlinearity phenomenon. Figure 7 depicts the performance comparison of the proposed S-EKF to PA and BPS DD-FL methods. Two most interesting scenarios for 64 subcarriers CO-OFDM transmission at 200 kHz combined laser linewidth, which are 4 inputs [Fig. 7(a)] and 8 inputs [Fig. 7(b)], are considered.

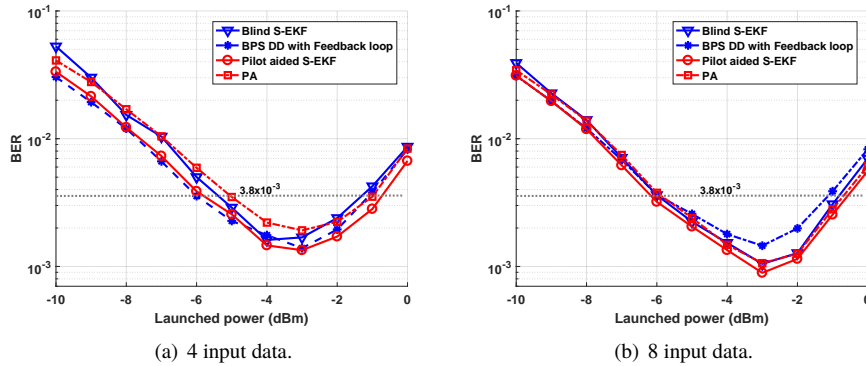


Fig. 7. The BER performance comparison of S-EKF with PA and BPS versus launched powers for 64 subcarriers 16QAM CO-OFDM fiber transmission at the distance of 1600 km (20 spans). The linewidth of transmitter and receiver lasers is 100 kHz.

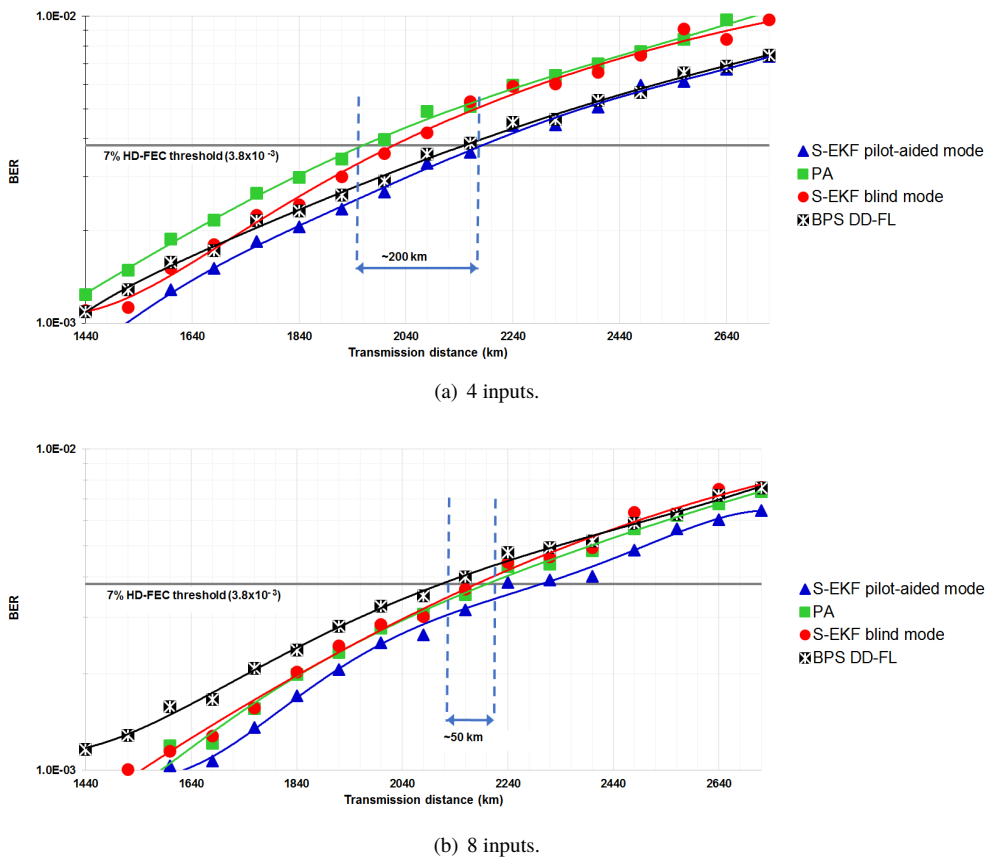


Fig. 8. The BER performance comparison of S-EKF with PA and BPS DD-FL versus transmission distance for 64 subcarriers 16QAM CO-OFDM systems at the optimum launched power of  $-3$  dBm. The linewidth of transmitter and receiver lasers is 100 kHz.

The transmission distance was kept at 1600 km (i.e. 20 spans) and the launched power was varied from  $-10$  dBm to 0 dBm. Similar trends are observed with fiber transmission from these two figures in which the system performance equipped with S-EKF increases according to increments of inputs. The optimum launched power for system with S-EKF is almost as the same as for the other methods, at around  $-3$  dBm. Nevertheless, the system equipped with S-EKF is slightly more sensitive to fiber nonlinearity than the two others when the launched power is above the optimum one. This, again, can be explained by the uncertainty noise increment due to fiber nonlinearity at high launched powers.

Finally, Fig. 8 shows the maximum transmission distance comparison between those PN compensation techniques at the HD-FEC threshold and at the optimum launched power of  $-3$  dBm. The number of inputs were unchanged. With 4 inputs [Fig. 8(a)], the pilot-aided mode S-EKF enhances transmission distance by  $\sim 200$  km in comparison with conventional PA method at the relatively same SE and complexity, while the blind mode S-EKF pushes the transmission distance  $\sim 50$  km further and provides at least ten times more computational efficiency than the complicated BPS DD-FL method with 8 inputs [Fig. 8(b)].

## 6. Conclusion

In this paper, we have reported the application of Kalman theory for CO-OFDM system to deal with phase noise compensation. We demonstrated that our proposed S-EKF outperformed the conventional PA and BPS DD-FL methods in terms of SE and computational complexity respectively for CO-OFDM systems with medium-sized subcarriers. At 200 kHz combined laser linewidth and at a launched power around  $-3$  dBm, the blind S-EKF with 8 inputs is strongly encouraged to apply for around 64-subcarriers 32 Gbaud 16-QAM CO-OFDM transmission to provide a high SE (no pilots used) and moderate low hardware complexity simultaneously.

## Funding

EU project ICONE (Grant No. 608099) in collaboration with Proximus SA, Belgium.